Hindawi Publishing Corporation
Advances in Mechanical Engineering
Article ID 792146

Research Article

Motion Structural Optimization Strategy for Rhombic Element Based Foldable Structure

Seung Hyun Jeong,[1] Jae Chung Heo,[1] and Gil Ho Yoon[2]

[1]*Graduate School of Mechanical Engineering, Hanyang University, Seoul 133-791, Republic of Korea*
[2]*School of Mechanical Engineering, Hanyang University, Seoul, Republic of Korea*

Correspondence should be addressed to Gil Ho Yoon; gilho.yoon@gmail.com

Received 22 October 2014; Accepted 9 December 2014

Academic Editor: Hae-Jin Choi

This research presents a new systematical design approach of foldable structure composed of several rhombic elements by applying genetic algorithm. As structural shapes represented by a foldable structure can be easily and dramatically morphed by manipulating rotational directions and angle of joints, the foldable structure has been used for various elementary structural members and engineering mechanisms. However a systematic design approach determining detail rotational angle and directions of unit cells for arbitrary shaped target areas has not been proposed yet. This research contributes to it by developing a new structural optimization method determining optimal angle and rotation directions to cover arbitrary shaped target areas of interest with aggregated rhombic elements. To achieve this purpose, we present an optimization formulation minimizing the sum of distances between each reference joint of an arbitrary shaped target area and its closest outer joints of foldable structure. To find out the outer joint set of a given foldable structure, an efficient geometric analysis method based on Delaunay triangulation is also developed and implemented. To show the validity and limitations of the present approach, several foldable structure design problems for two-dimensional arbitrary shaped target areas are solved with the present optimization procedure.

1. Introduction

This study presents a new systematic design approach of foldable structure or mechanism covering arbitrary shaped target areas. Foldable structure can be constructed simply with repeated unit cells composed of rigid links, ropes, revolute, pivot joints, and scissor hinges; for an example, Figure 1 shows a typical example of a foldable structure—a luggage elevator used in airport. Due to its simplicity in designing and manufacturing, foldable structure has been used in many studies for various engineering applications such as temporary protective covers, antennas and radio towers, emergency shelters, lightweight camping, bridges, hospital, and other public buildings. Some benefits of foldable structure from an engineering point of view may be the fastness, the easiness in deployment and transportation, and the deformability in terms of geometry (morphing from one structure to anther shape structure). In short the simplicity and the deformability of a folding structure or a mechanism regardless of construction site are important features and characteristics of folding mechanism. Nevertheless except some popular and available folding structures, it is often difficult to determine the configuration parameters such as angle and rotation direction of folding structure. In other words, it is not straightforward in determining the geometric parameters of relative complex folding structure. To contribute this aspect, this research tries to develop a new systematic design optimization approach to improve the deformability of folding mechanism to cover arbitrary shaped target areas or to be installed at any construction site.

To design an optimal repeated internal unit cell or a foldable structure, a number of studies have been carried out (see [1–6] and the references therein). You and Pellegrino presented a new general type of two-dimensional foldable structure [1]. Benjeddou et al. presented an innovative concept of a foldable composite beam made of wooden blocks [2]. Zanardo illustrated a new concept of the geometry and the kinematics of two articulated systems [3]. Hoberman developed a new simpler angulated element consisting of rods and scissor hinges and presented many applications

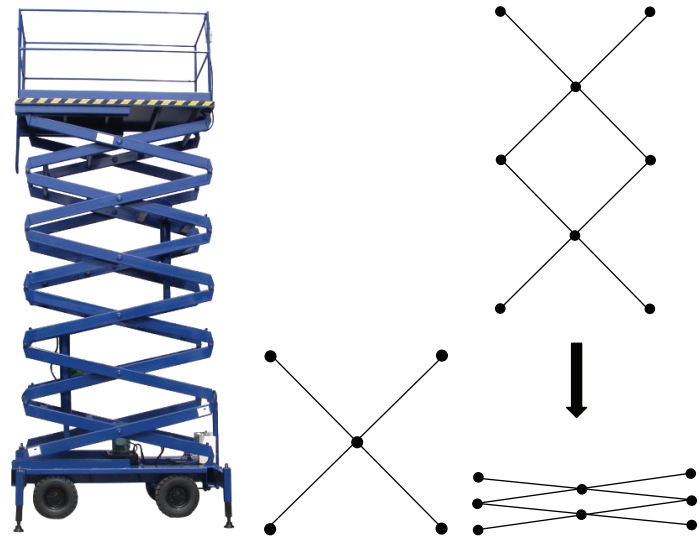

Figure 1: Luggage elevation foldable structure. (a) An example of a foldable structure in airport luggage elevation, (b) a unit cell of the foldable structure, and (c) an elementary structure with rigid links and joints for the foldable structure of (a).

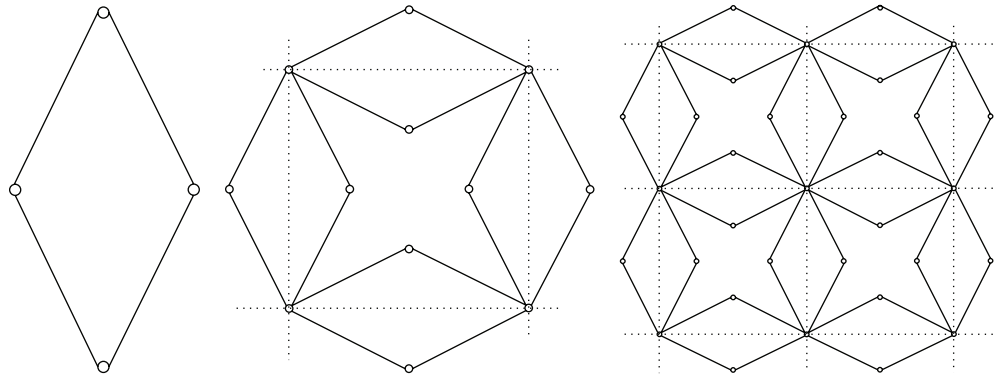

Figure 2: (a) Unit cell of foldable structure considered in this research, (b) 4RE-linkage, and (c) 2 by 2 foldable structure.

of their foldable structures [4–6]. Viquerat et al. used a plane symmetric Bricard linkage for developing a deployable structure and the internal mechanism of the structure is described in terms of its Denavit-Hartenberg parameters [7]. Based on the mechanism theory, Zhao et al. investigated the application of deployable structure (folding structure) based on scissor-like element (SLE) for a foldable stair [8, 9]. Also Cai et al. studied Hoberman's linkage [10] and Kempe suggested a new foldable structure using four-piece linkage [11]. From our review of these literatures, it is found that although many analytical and numerical methods have been proposed to design a unit cell of folding structure, there are few design approaches concerning how to assemble unit cells and how to determine geometric configuration parameters (angle and positions) to cover arbitrary shaped areas. For a practical example, let us assume that we need to repair some destroyed parts of space shuttle, nuclear power plants, oil pipe in deep sea, or submarine pipeline without waste of time and risk factor [12, 13]. Without knowing the shape or area of damaged part, a robot without multihazard risk to human life can be urgently deployed in space, damaged nuclear power plant, or damaged parts of deep sea and it can take emergency measures with foldable structures before permanent repairmen. But in those emergency situations, often the shapes and conditions of damages are unknown that makes it hard to repair damages. Therefore we have a plan to make an intelligent and robust robot that can detect shapes of destroyed parts with IR image cameras or electromagnetic sensors and can make fundamental frames with folding structures with artificial intelligence for the sake of sealing and contaminated water-drainage. This kind of technology has been also important after the accident of nuclear power plants in Russia and Japan and to every country having submarines, nuclear power plants, or space satellites. Here it should be noticed that the shape or area of destroyed parts is now known a priori. It is our proposition that even in

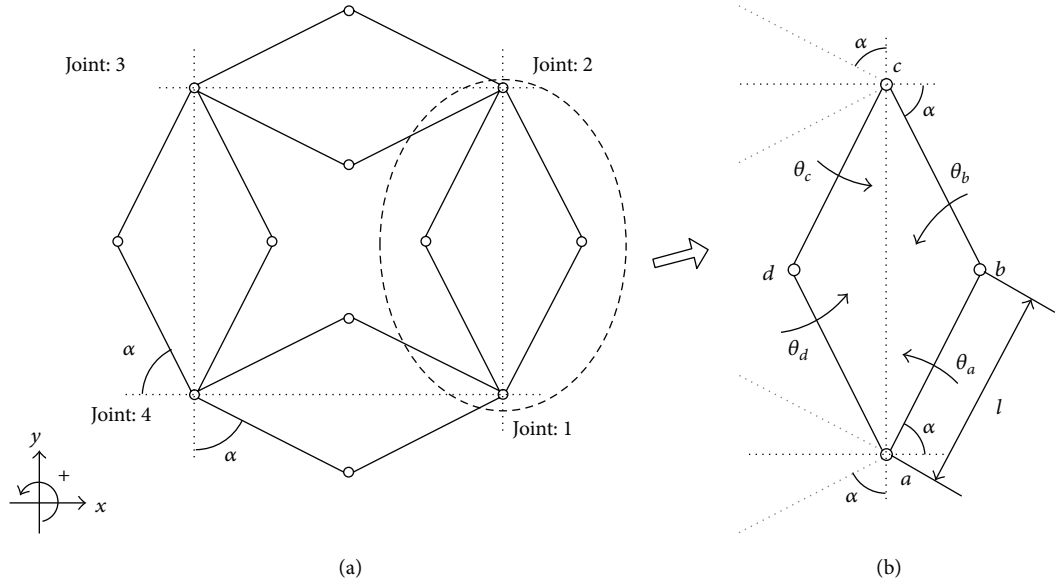

Figure 3: A repeated building block: 4RE linkage. (a) A repeated mechanism building block (4RE linkage consisting of 4 rhombic elements) and (b) a representing rhombic element and its geometric notations.

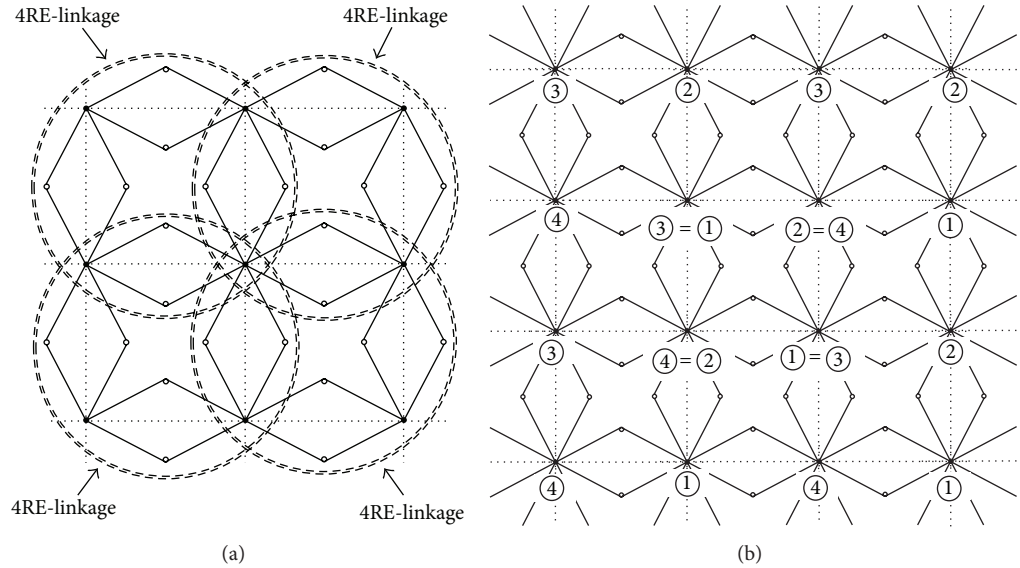

Figure 4: The assembling repeated building block. (a) The foldable structure consisted of the 4RE linkage and (b) the repetitive manner to construct a foldable structure.

these situations, with the help of the deformability of folding structure, a robot can deliver some standard basic folding mechanisms with repeated unit cells, that is, 2 by 2 or 3 by 3 folding structure, and the present design approach can be used to determine the geometric configuration parameters which make the folding mechanisms fit to target holes and the robot can imminently repair the breakdowns.

To develop a systematic design method, the geometric configuration called a rhombic element of Figure 2(a) proposed by Tanaka et al. [14] in Figure 2 is considered. In Figure 2, the assembly of 4 rhombic elements of Figure 2(b) is called 4RE-linkage and the assembly of four 4RE-linkages is called a 2 by 2 foldable structure. In their study, they focused on establishing the relationship between the overall deformability and the spatial location of planar structure. As an extension to these relevant researches, this study focuses on how to efficiently and effectively determine the geometric configuration parameters to adjust the outline shape of a foldable structure especially for arbitrary shaped areas. As the optimization problem is inherently nonlinear and has many local optima, the genetic algorithm method becomes a natural choice in this study. Specifically the rotational directions of joints and their magnitudes are parameterized by binary design variables (0 or 1) and integer variables, respectively.

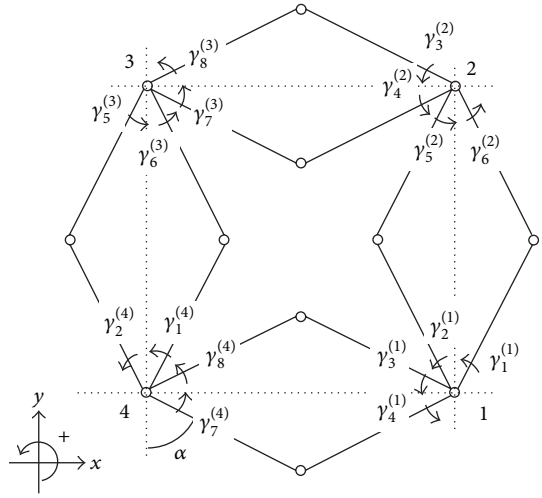

Figure 5: A 4RE-linkage: repeated rhombic blocks. (Note that the rotational angles are denoted by $\gamma_i^{(j)}$ for the rotational angle of the ith joint of the jth link rather than θ in (4).)

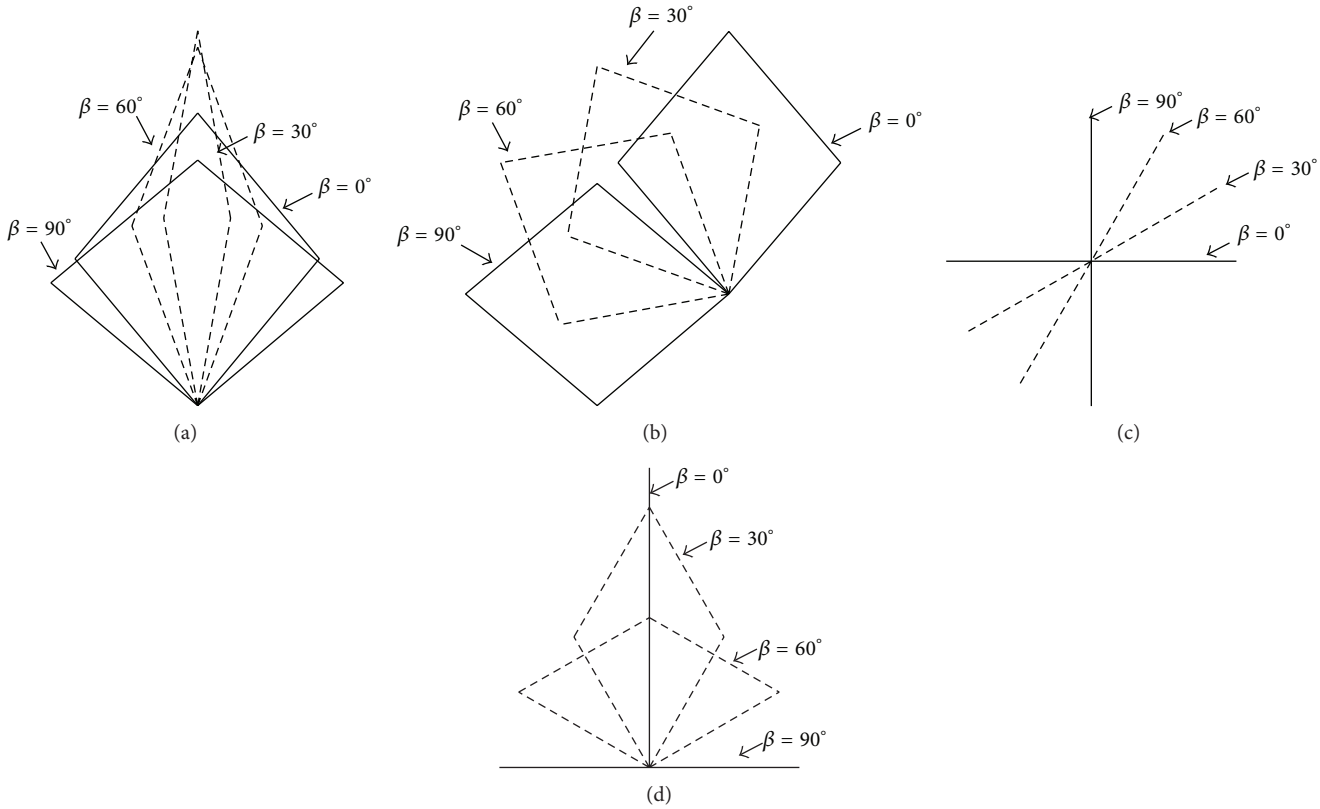

Figure 6: Several motions of a rhombic element. (a) The structures with the mode = [+1 +1 +1 +1] and $\beta = 0^\circ, 30^\circ, 60^\circ, 90^\circ$, (b) the structures with the mode = [+1 −1 +1 −1] and $\beta = 0^\circ, 30^\circ, 60^\circ, 90^\circ$, (c) the structures with the mode = [+1 +1 −1 −1] and $\beta = 0^\circ, 30^\circ, 60^\circ, 90^\circ$, and (d) the structures with the mode = [+1 −1 −1 +1] and $\beta = 0^\circ, 30^\circ, 60^\circ, 90^\circ$.

From an optimization point of view, the objective function is set to the sum of distances between each reference point and its closest outer node point of a foldable structure of interest. If the objective value is converged to zero, in principle the foldable structure with the optimized design variables can exactly fit the outlines of the arbitrary shape areas of interest.

To our best knowledge, however, it is found that it becomes a tricky task to determine the outer joints defining the outline of the foldable structure as a set of its outer joints is subject to be changed. In order to determine the set of outer joint points, this research presents a new numerical approach based on the Delaunay triangulation method [15].

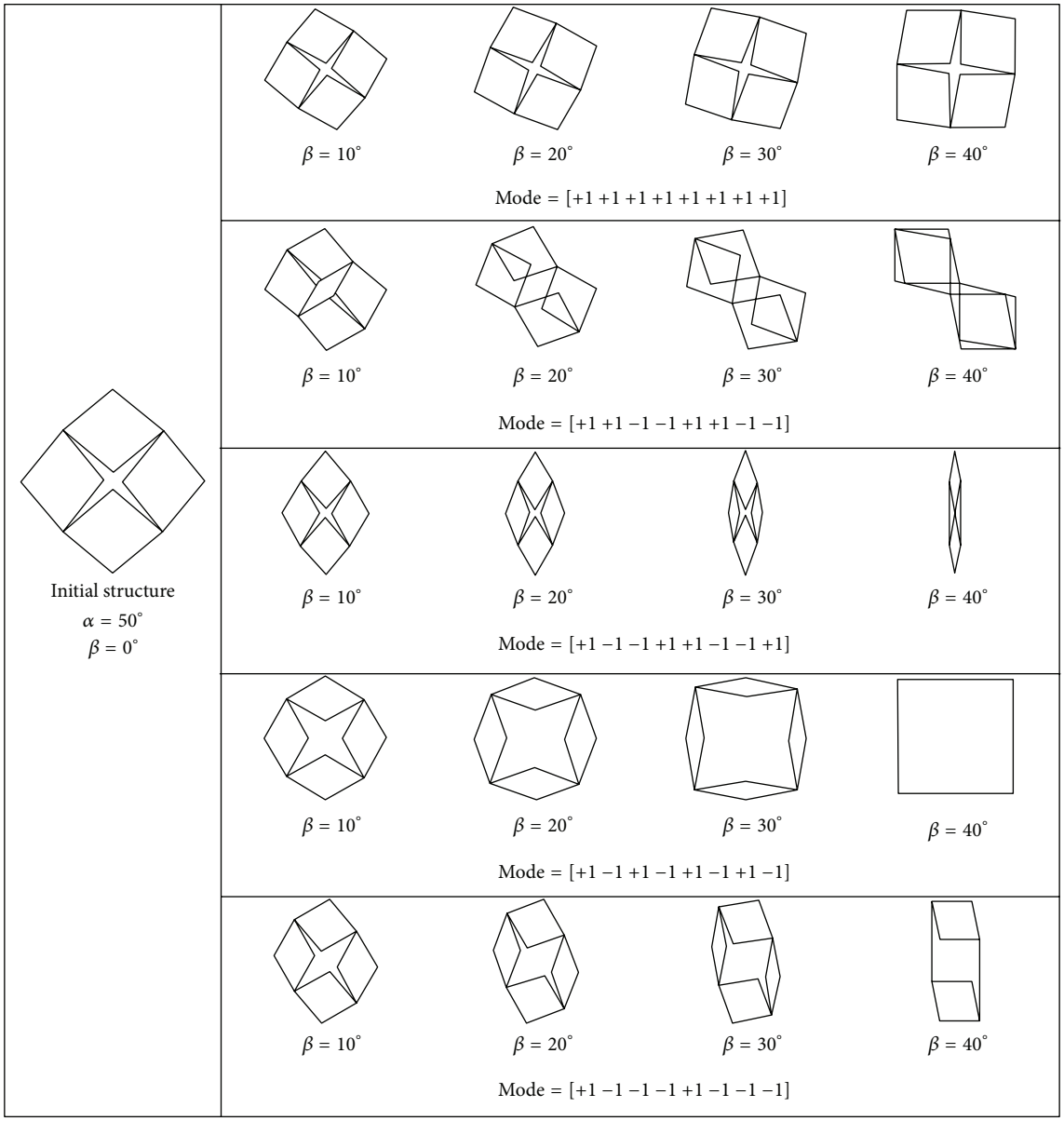

Figure 7: Several motions of 4RE-linkages using $\alpha = 50^\circ$ and five different modes.

This paper is organized as follows. The basic kinematic analysis of foldable structure which is composed of repeated unit cell of rigid-body mechanism is given in Section 2. A parameterization based on the kinematic analysis and a new optimization problem formulation using binary and integer design variables are described in Section 3. In Section 4, several numerical examples of designing foldable structure are presented to validate the proposed design approach. Finally, our findings and new topics for further research are discussed and summarized.

2. Kinematic Analysis of Four Rhombic Elements Based Foldable Structure

Figure 3 shows the four-rhombic-element linkage (4RE-linakge) formed by 16 equilateral and rectilinear bars for 4 unit cells [14]. The 16 identical straight bars are connected for eight 2-bar and for four 4-bar linkages. Due to the simplicity of the 4RE-linkage in geometry as well as in manufacturing, it has been used as a basic constructing element for a various engineering structures by changing its geometrical configuration [14]. To explore its versatility from a geometric point of view, the kinematic analysis of 4RE-linkage can be conducted as shown in Figure 3.

2.1. Kinematic Analysis of a Rhombic Element. Note that the kinematic analysis of a basic rhombic element in Figure 3(b) provides some essential mathematical and theoretical foundations in utilizing the various rigid body motions of various foldable structures. Obviously the basic geometric configuration of the rhombic element is determined by the length

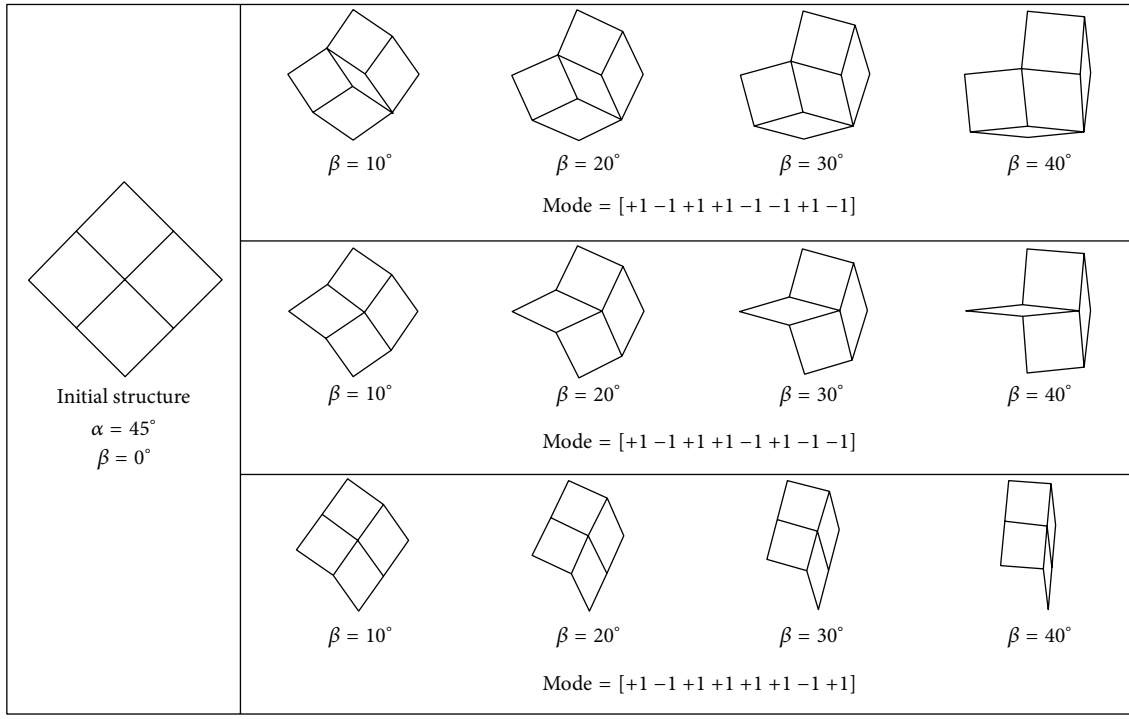

Figure 8: Several motion of 4RE-linkages using $\alpha = 45^\circ$ and three different modes.

of rigid bar l and the angle α of the component links (see Figure 3(b)). An investigation of the rhombic element of Figure 3(b) turns out a loop close equation, $\overrightarrow{ab} + \overrightarrow{bc} + \overrightarrow{cd} + \overrightarrow{da} = 0$, for one of the essential kinematic analyses with the geometrical constraint conditions, that is, $\overline{ab} = \overline{bc} = \overline{cd} = \overline{ca} = l$ and $\angle abc = \angle cda = 2\alpha$. This closed loop vector equation turns out the two-component equations according to x-axis and y-axis as follows:

$$\begin{aligned} x\text{: } & l\cos(\theta_a + \alpha) + l\cos(\theta_b - \alpha + \pi) + l\cos(\theta_c + \alpha + \pi) \\ & + l\cos(\theta_d - \alpha) = 0, \\ y\text{: } & l\sin(\theta_a + \alpha) + l\sin(\theta_b - \alpha + \pi) + l\sin(\theta_c + \alpha + \pi) \\ & + l\sin(\theta_d - \alpha) = 0. \end{aligned} \tag{1}$$

For the sake of simplicity, (1) can be rearranged in terms of the rotational angle α:

$$\begin{aligned} x\text{: } & \cos\alpha(\cos\theta_a - \cos\theta_b - \cos\theta_c + \cos\theta_d) \\ & + \sin\alpha(-\sin\theta_a - \sin\theta_b + \sin\theta_c + \sin\theta_d) = 0, \\ y\text{: } & \cos\alpha(\sin\theta_a - \sin\theta_b - \sin\theta_c + \sin\theta_d) \\ & + \sin\alpha(\cos\theta_a + \cos\theta_b - \cos\theta_c - \cos\theta_d) = 0. \end{aligned} \tag{2}$$

From the above two geometric compatibility conditions, an important notation of rotational modes regardless of the rotational angle α in the range from 0 to $\pi/2$ can be introduced in [14]:

$$\begin{aligned} \theta_a = \theta_c, \quad \theta_b = \theta_d, \quad 0 < \alpha < \frac{\pi}{2}, \\ \theta_a + \theta_d = \theta_b + \theta_c, \quad \alpha = 0, \\ \theta_a + \theta_b = \theta_c + \theta_d, \quad \alpha = \frac{\pi}{2}. \end{aligned} \tag{3}$$

The above geometric compatibility conditions, (3), result in the following 4 rotational modes of the rhombic element [14]:

$$\begin{aligned} \boldsymbol{\theta} &= \{\theta_a \ \ \theta_b \ \ \theta_c \ \ \theta_d\} \\ &= \begin{cases} \boldsymbol{\theta}_0 = \{+1, +1, +1, +1\}, & 0 < \alpha < \dfrac{\pi}{2}, \\ \boldsymbol{\theta}_1 = \{+1, -1, +1, -1\}, & 0 < \alpha < \dfrac{\pi}{2}, \\ \boldsymbol{\theta}_2 = \{+1, +1, -1, -1\}, & \alpha = 0, \\ \boldsymbol{\theta}_3 = \{+1, -1, -1, +1\}, & \alpha = \dfrac{\pi}{2}, \end{cases} \end{aligned} \tag{4}$$

where the four rotational modes are denoted by $\boldsymbol{\theta}_0$, $\boldsymbol{\theta}_1$, $\boldsymbol{\theta}_2$, and $\boldsymbol{\theta}_3$, respectively. With the rotational modes, the motion of a rhombic element can be expressed as a scaled sum of the four rotational modes. In each rotational mode, the rotational direction is either counterclockwise (+1) or clockwise (−1). It is worthy to notice that the above four rotational modes and their notations become bases to analyze the motion of 4RE-linkage.

2.2. Kinematic Analysis of 4RE-Linkage. Based on the notations and the analysis procedures for the RE in the precedent section, the kinematic analysis procedure and the planar

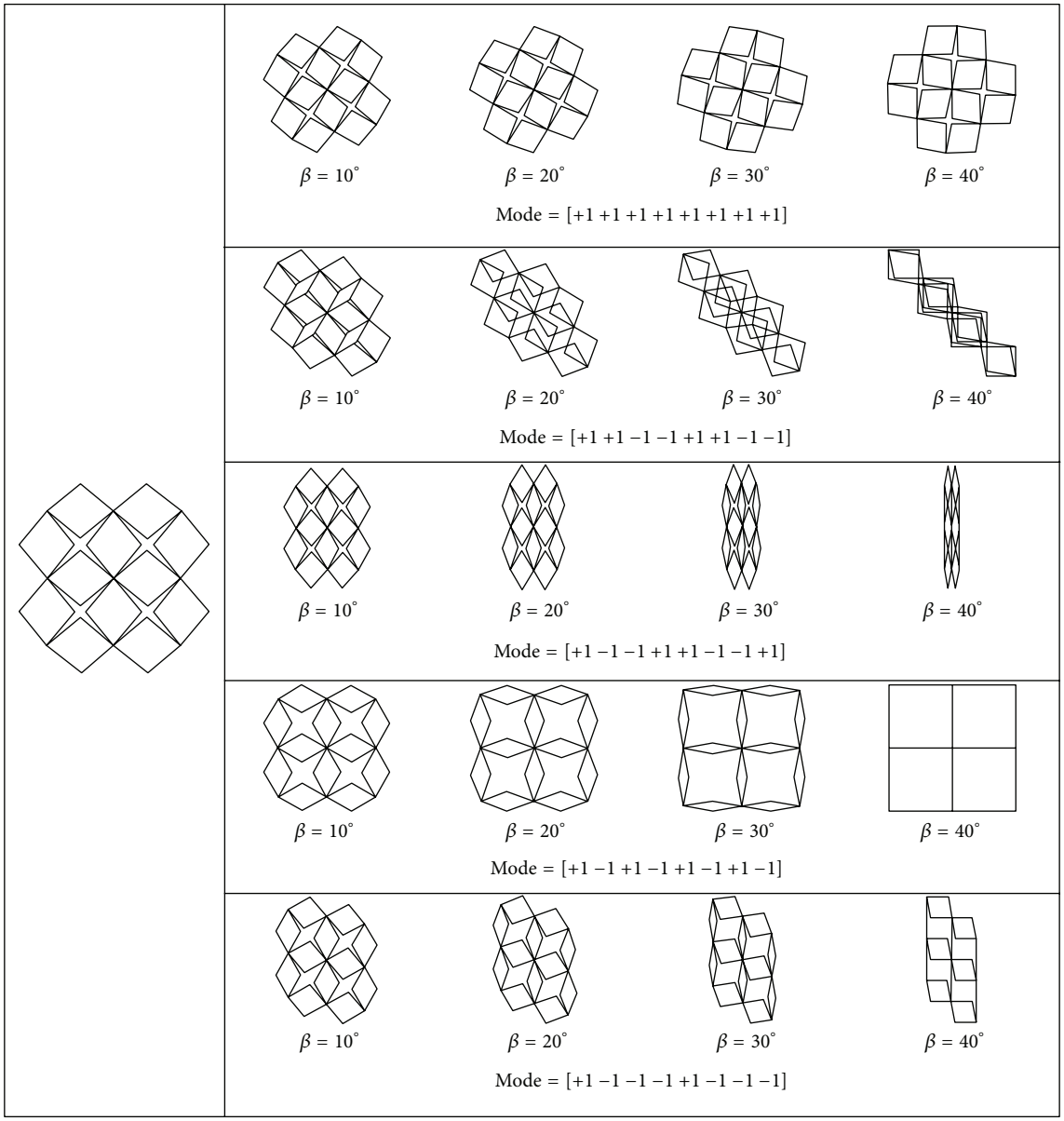

Figure 9: Several motions of foldable structure assembled by 2 by 2 4RE-linkages using $\alpha = 50^\circ$ and five different modes.

deformation mobility of the foldable structure of Figure 5 can be analyzed similarly [14]. Refer to Figure 5 for the angle notations employed for the 4RE-linkage.

As this foldable structure consists of the 4 rhombic elements of Figure 4, the rotational parameters can be defined. In Figure 4(b), the repetitive assemblage can be defined by attaching the joint 1 of one repeated building block to the joint 3 of an adjacent repeated building block. Similar to this, the joint 2 can be attached to the joint 4 of an adjacent repeated building block:

$$x\colon h\left(\frac{\gamma_1^{(1)}-\gamma_2^{(1)}}{2}\right)\cos\left(\frac{\gamma_1^{(1)}+\gamma_2^{(1)}}{2}+\frac{\pi}{2}\right)+h\left(\frac{\gamma_3^{(2)}-\gamma_4^{(2)}}{2}\right)\cos\left(\frac{\gamma_3^{(2)}+\gamma_4^{(2)}}{2}+\pi\right)+h\left(\frac{\gamma_5^{(3)}-\gamma_6^{(3)}}{2}\right)\cos\left(\frac{\gamma_5^{(3)}+\gamma_6^{(3)}}{2}+\frac{3\pi}{2}\right)+h\left(\frac{\gamma_7^{(4)}-\gamma_8^{(4)}}{2}\right)\cos\left(\frac{\gamma_7^{(4)}+\gamma_8^{(4)}}{2}\right)=0,$$

$$y\colon h\left(\frac{\gamma_1^{(1)}-\gamma_2^{(1)}}{2}\right)\sin\left(\frac{\gamma_1^{(1)}+\gamma_2^{(1)}}{2}+\frac{\pi}{2}\right)+h\left(\frac{\gamma_3^{(2)}-\gamma_4^{(2)}}{2}\right)\sin\left(\frac{\gamma_3^{(2)}+\gamma_4^{(2)}}{2}+\pi\right)$$

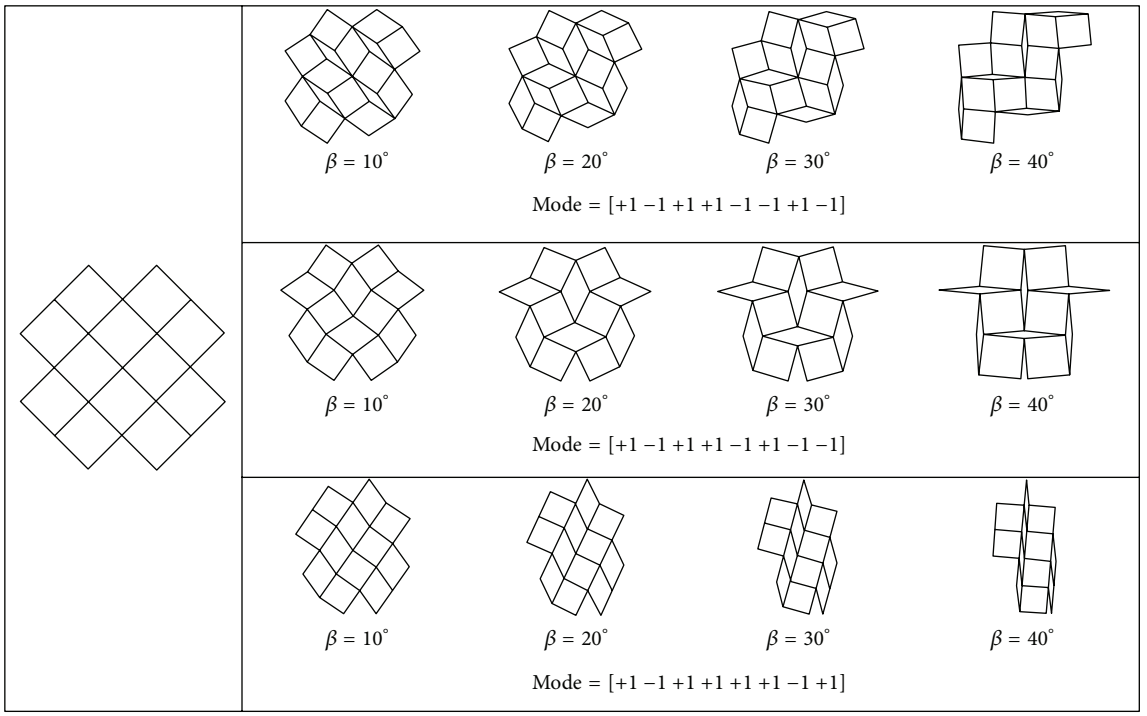

Figure 10: Motions of foldable structure assembled by 2 by 2 4RE-linkages using $\alpha = 45^\circ$ and three different modes.

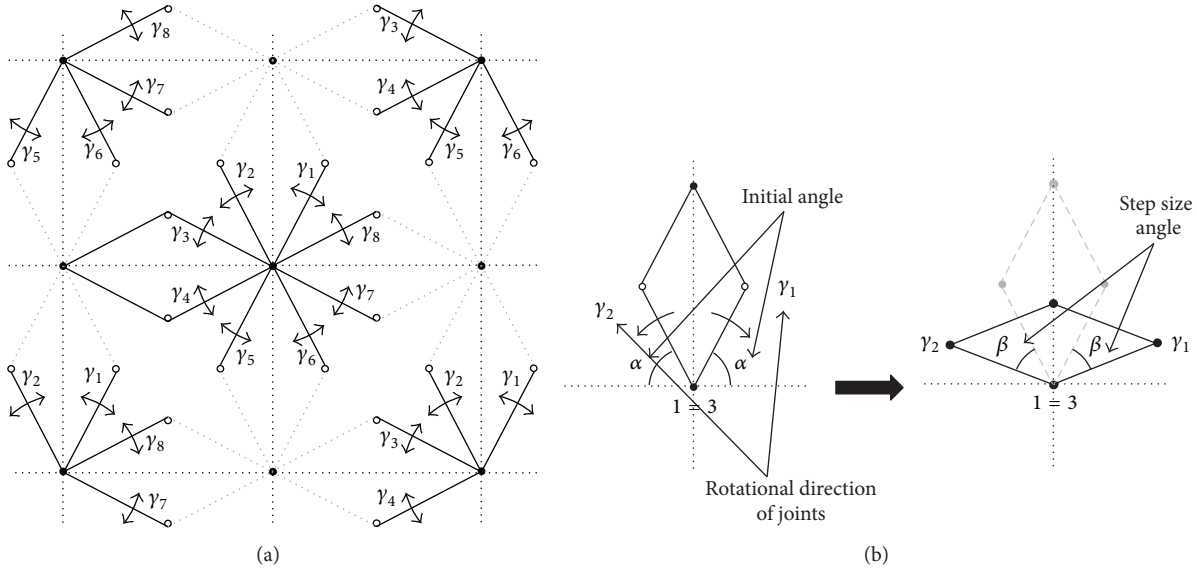

Figure 11: Parameterization of the rotational direction of joints and the magnitude of the angle. (a) A rotational direction of joints and (b) the magnitude of the joint angle.

$$+ h\left(\frac{\gamma_5^{(3)} - \gamma_6^{(3)}}{2}\right)\sin\left(\frac{\gamma_5^{(3)} + \gamma_6^{(3)}}{2} + \frac{3\pi}{2}\right)$$
$$+ h\left(\frac{\gamma_7^{(4)} - \gamma_8^{(4)}}{2}\right)\sin\left(\frac{\gamma_7^{(4)} + \gamma_8^{(4)}}{2}\right) = 0, \quad (5)$$

where $\gamma_i^{(j)}$ represents the rotational angle of the ith joint of the jth link in Figure 5 and h is a function of the segment $\overline{ac}$ in Figure 3(b) and is given as follows:

$$h(t) = 2l\sin(\alpha + t). \quad (6)$$

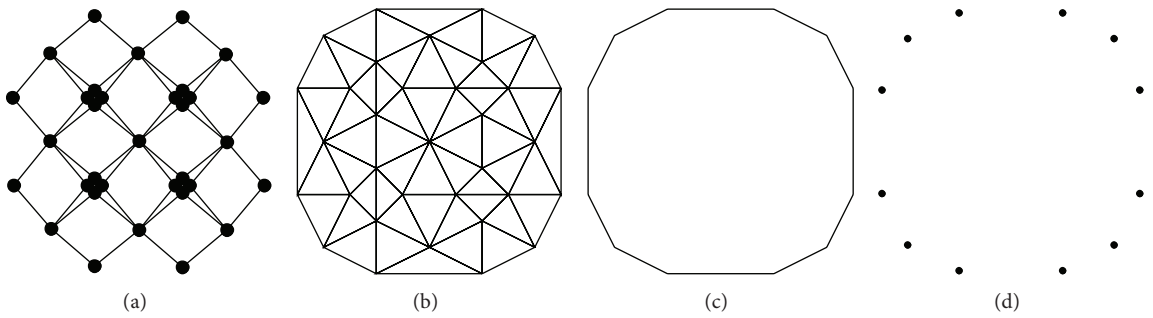

Figure 12: An example of the outer joint detection process during optimization. (a) A given foldable structure, (b) a Delaunay triangulation of the structure, (c) the boundary edges extracted from the Delaunay triangulation, and (d) the outer nodes from the boundary edges.

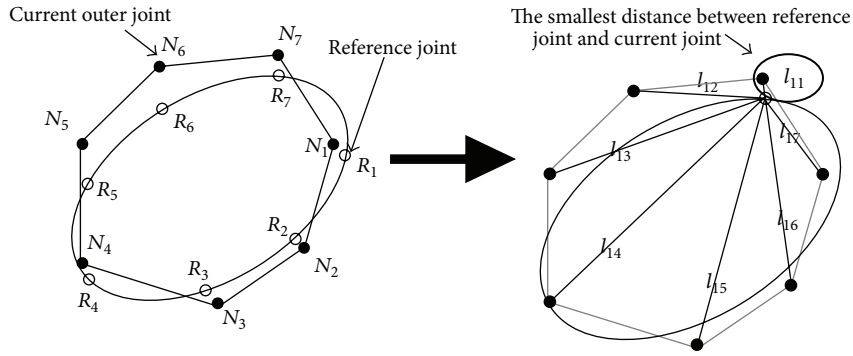

Figure 13: The meanings of the distances and the objective function (the reference joint and the current outer joint are denoted by R_i and N_j, resp.).

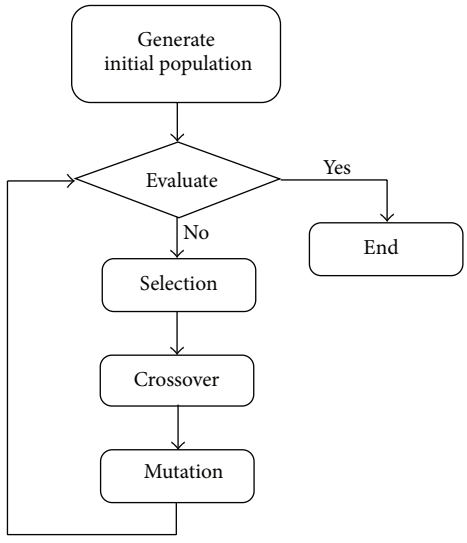

Figure 14: Flow chart of the genetic algorithm.

Similar to the kinematic analysis for the rhombic element, (5) can be rearranged in terms of α in $0 \le \alpha \le \pi/2$ to find out its rotational modes as follows:

$$\begin{aligned} x:\ & \sin\alpha\left(-\sin\gamma_1^{(1)} - \sin\gamma_2^{(1)} - \cos\gamma_3^{(2)} - \cos\gamma_4^{(2)} + \sin\gamma_5^{(3)}\right. \\ & \left. + \sin\gamma_6^{(3)} + \cos\gamma_7^{(4)} + \cos\gamma_8^{(4)}\right) \\ & + \cos\alpha\left(\cos\gamma_1^{(1)} - \cos\gamma_2^{(1)} - \sin\gamma_3^{(2)} + \sin\gamma_4^{(2)} - \cos\gamma_5^{(3)}\right. \\ & \left. + \cos\gamma_6^{(3)} + \sin\gamma_7^{(4)} - \sin\gamma_8^{(4)}\right) = 0, \\ y:\ & \sin\alpha\left(\cos\gamma_1^{(1)} + \cos\gamma_2^{(1)} - \sin\gamma_3^{(2)} - \sin\gamma_4^{(2)} - \cos\gamma_5^{(3)}\right. \\ & \left. - \cos\gamma_6^{(3)} + \sin\gamma_7^{(4)} + \sin\gamma_8^{(4)}\right) \\ & + \cos\alpha\left(\sin\gamma_1^{(1)} - \sin\gamma_2^{(1)} + \cos\gamma_3^{(2)} - \cos\gamma_4^{(2)} - \sin\gamma_5^{(3)}\right. \\ & \left. + \sin\gamma_6^{(3)} - \cos\gamma_7^{(4)} + \cos\gamma_8^{(4)}\right) = 0. \end{aligned} \tag{7}$$

By analyzing (7), the following geometric constraints can be obtained:

$$\begin{aligned} & \gamma_1^{(1)} = \gamma_5^{(3)}, \quad \gamma_2^{(1)} = \gamma_6^{(3)}, \quad \gamma_3^{(2)} = \gamma_7^{(4)}, \quad \gamma_4^{(2)} = \gamma_8^{(4)}, \quad \forall\alpha \\ & \gamma_1^{(1)} + \gamma_8^{(4)} = \gamma_4^{(2)} + \gamma_5^{(3)}, \quad \gamma_2^{(1)} + \gamma_3^{(2)} = \gamma_6^{(3)} + \gamma_7^{(4)}, \quad \alpha = \frac{\pi}{4}. \end{aligned} \tag{8}$$

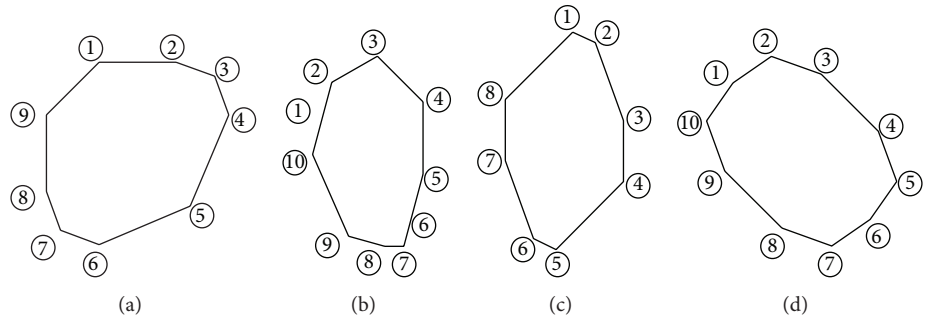

Figure 15: Four target areas of interest for the 2 by 2 foldable mechanism. (a) Target area 1 ($\mathbf{x}^* = [1, 0, 1, 45, 25]$), (b) target area 2 ($\mathbf{x}^* = [1, 1, 1, 45, 30]$), (c) target area 3 ($\mathbf{x}^* = [1, 0, 0, 15, 25]$), and (d) target area 4 ($\mathbf{x}^* = [0, 0, 1, 35, 20]$) for the 2 by 2 foldable structure.

Then the following 8 rotational modes from γ_0 to γ_8 can be obtained for the 4RE-linkage as follows:

$$\boldsymbol{\gamma} = \left\{\gamma_1^{(1)} \;\; \gamma_2^{(1)} \;\; \gamma_3^{(2)} \;\; \gamma_4^{(2)} \;\; \gamma_5^{(3)} \;\; \gamma_6^{(3)} \;\; \gamma_7^{(4)} \;\; \gamma_8^{(4)}\right\}$$

$$= \begin{cases} \boldsymbol{\gamma}_0 = \{+1 \;\; +1 \;\; +1 \;\; +1 \;\; +1 \;\; +1 \;\; +1 \;\; +1\}, & \forall\alpha \\ \boldsymbol{\gamma}_1 = \{+1 \;\; +1 \;\; -1 \;\; -1 \;\; +1 \;\; +1 \;\; -1 \;\; -1\}, & \forall\alpha \\ \boldsymbol{\gamma}_2 = \{+1 \;\; -1 \;\; -1 \;\; +1 \;\; +1 \;\; -1 \;\; -1 \;\; +1\}, & \forall\alpha \\ \boldsymbol{\gamma}_3 = \{+1 \;\; -1 \;\; +1 \;\; -1 \;\; +1 \;\; -1 \;\; +1 \;\; -1\}, & \forall\alpha \\ \boldsymbol{\gamma}_4 = \{+1 \;\; -1 \;\; -1 \;\; -1 \;\; +1 \;\; -1 \;\; -1 \;\; -1\}, & \forall\alpha \\ \boldsymbol{\gamma}_5 = \{+1 \;\; -1 \;\; +1 \;\; +1 \;\; -1 \;\; -1 \;\; +1 \;\; -1\}, & \alpha = \dfrac{\pi}{4} \\ \boldsymbol{\gamma}_6 = \{+1 \;\; -1 \;\; +1 \;\; +1 \;\; -1 \;\; +1 \;\; -1 \;\; -1\}, & \alpha = \dfrac{\pi}{4} \\ \boldsymbol{\gamma}_7 = \{+1 \;\; -1 \;\; +1 \;\; +1 \;\; +1 \;\; +1 \;\; -1 \;\; +1\}, & \alpha = \dfrac{\pi}{4}. \end{cases} \tag{9}$$

Any motion of the 4RE-linkage can be described by the scaled sum of the rotational modes of (9).

2.3. Complex Motions of a Foldable Structure

2.3.1. Rhombic Element and 4RE-Linakge. This subsection aims to show that it is tedious and difficult to predict the motions of the rhombic element, that is, the 4RE-linkage and the foldable structure (here 2 by 2 4RE-linkage) with the given geometric parameters. First of all, as studied there are only the four rotational modes for the rhombic element of Figure 6. The motions can be visualized easily by using few modes and rotational angle of the rhombic element. For an example, Figure 6 shows some motions of the rhombic element according to the changes of a step size angle β with an arbitrarily chosen 50 degrees for α. Here all the step size angles of the links are set to β and the rotational angle can be expressed as follows:

$$\boldsymbol{\theta} = \{\theta_a, \theta_b, \theta_c, \theta_d\}$$
$$= \{\beta, \beta, \beta, \beta\} = \beta\boldsymbol{\theta}_0 \quad (\boldsymbol{\theta}_0\text{: the first rotational mode}). \tag{10}$$

As the motion of the rhombic element is under the pure rotation with β degrees, it is easy to describe and visualize. On the other hand, Figure 7 represents the five rotational modes of the 4RE-linkage with $\alpha = 50^\circ$ and Figure 8 represents three rotational modes of 4RE-linkage with $\alpha = 45^\circ$. As shown, the motions of 4RE-linkages become more complicated than the case of one rhombic element.

2.3.2. 2 by 2 Foldable Structure. To show a more complex case, we constructed 2 by 2 foldable structure first. By setting $\alpha = 50^\circ$ in Figure 9 and $\alpha = 45^\circ$ in Figure 10, several rotational modes are plotted with some arbitrarily chosen step angle, β. See that while the motions of the 2 by 2 foldable structure with $\alpha = 50^\circ$ can be predicted because they are similar to the motions of 4RE-linkages, the motions with $\alpha = 45^\circ$ are almost impossible to predict by just observing the shapes of 4RE-linkages. In short, through the observations of the motions of the rhombic element, the 4RE-linkage, and a 2 by 2 foldable structure, it is nearly impossible to predict and design the motions of an arbitrary foldable structure by engineer's intuition. It is our proposition that a systematic design approach is required and the next sections will develop a new method and prove its validity in designing several structures. In addition, it should be mentioned that, as described in [14], mechanisms can be assembled with special joints and rigid bars. For example, when a mechanism has 45 degrees for $\alpha+\beta$ as shown in Figures 8 and 10, the overlapping between rhombic elements occurs. To avoid overlapping, some special type joints should be adopted. Refer to [14] for the assemblage without the overlapping among components.

3. Structure Optimization Formulation for Foldable Structure

In Section 2, the assemblages of some element building blocks show complex movements and their covered areas are subject to be changed dramatically by changing their geometric parameters, that is, the rotational direction and the magnitudes of angles of rigid bars. From an engineering point of view, this geometric feature can be exploited for various engineering purposes such as the application of robotic movement for complex and undetermined hazard environments, the application for the structural damage management of a larger structure, or just the application of toy.

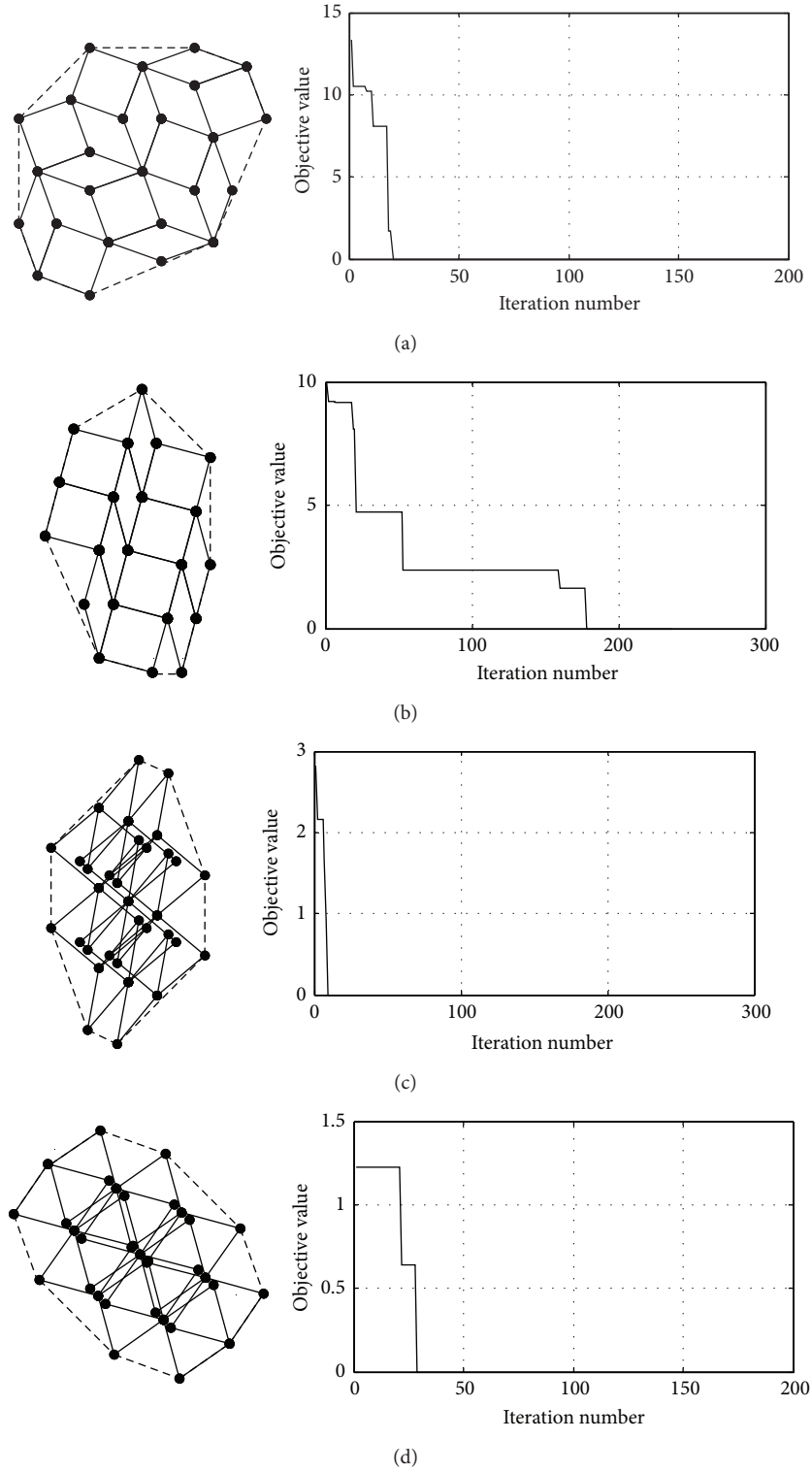

Figure 16: Optimization results for a 2 by 2 foldable structure. (a) An optimized foldable structure for the target area 1 and its convergence history ($\mathbf{x} = [1, 0, 1, 45, 25]$), (b) an optimized foldable structure for the target area 2 and its convergence history ($\mathbf{x} = [1, 1, 1, 45, 30]$), (c) an optimized foldable structure for the target area 3 and its convergence history ($\mathbf{x} = [1, 0, 0, 15, 25]$), and (d) an optimized foldable structure for the target area 4 and its convergence history ($\mathbf{x} = [0, 0, 1, 35, 20]$).

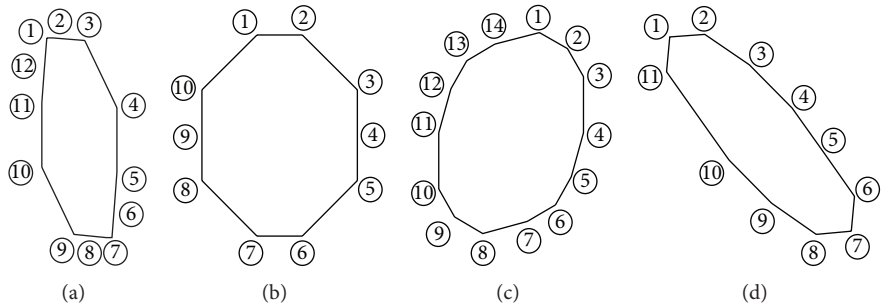

Figure 17: Four target areas of interest for the 3 by 2 foldable mechanism. (a) Target area 1 ($\mathbf{x}^* = [1, 1, 1, 45, 40]$), (b) target area 2 ($\mathbf{x}^* = [0, 1, 1, 30, 5]$), (c) target area 3 ($\mathbf{x}^* = [1, 0, 1, 45, 15]$), and (d) target area 4 ($\mathbf{x}^* = [0, 0, 1, 50, 35]$) for the 3 by 2 foldable structure.

We also notice that the predictions of the mobility and the covered shape of a foldable structure are tedious and heuristic. Therefore it is preferred to develop a systematic and robust design approach based on some engineering optimization theories for this purpose. By detecting and measuring the approximated shapes of areas and applying a systematic and robust design approach to determine the geometric parameters of a basic foldable structure, we can obtain the geometric parameters of the foldable structure to make its shape fitted to target shapes. To do this, at first we define the binary and the integer design variables for the rotational directions of joints and the magnitudes of angles. To make the shape of a foldable structure to a shape of interest matched, the optimization method presented in this research can be applied. Here it was an important issue to efficiently classify joints defining the outline of a foldable structure.

3.1. Parameterizations of Rotational Direction of Joints and Magnitudes of Rotation Angles. The rotational directions of joints and the magnitudes of angles in Figure 11 are parameterized with the binary and the integer design variables, respectively. Because there are eight rotational modes of the considered foldable structure, three-digit binary design variable is needed to represent the rotational modes. The three-digit binary design variable will represent eight rotational modes as follows. The design variable can be represented by the integer design variable range from 1 to 8 naturally; however, the binary design variable is used in this research:

$$\mathbf{r} = \{r_1 \;\; r_2 \;\; r_3\} \Longrightarrow \boldsymbol{\gamma} = \{\gamma_1 \;\; \gamma_2 \;\; \gamma_3 \;\; \gamma_4 \;\; \gamma_5 \;\; \gamma_6 \;\; \gamma_7 \;\; \gamma_8\}$$

$$\text{if } \mathbf{r} = \{0 \;\; 0 \;\; 0\},$$

$$\text{then } \boldsymbol{\gamma} = \boldsymbol{\gamma}_0 = \{+1 \;\; +1 \;\; +1 \;\; +1 \;\; +1 \;\; +1 \;\; +1 \;\; +1\}$$

$$\text{if } \mathbf{r} = \{0 \;\; 0 \;\; 1\},$$

$$\text{then } \boldsymbol{\gamma} = \boldsymbol{\gamma}_1 = \{+1 \;\; +1 \;\; -1 \;\; -1 \;\; +1 \;\; +1 \;\; -1 \;\; -1\}$$

$$\text{if } \mathbf{r} = \{0 \;\; 1 \;\; 0\},$$

$$\text{then } \boldsymbol{\gamma} = \boldsymbol{\gamma}_2 = \{+1 \;\; -1 \;\; -1 \;\; +1 \;\; +1 \;\; -1 \;\; -1 \;\; +1\}$$

$$\text{if } \mathbf{r} = \{0 \;\; 1 \;\; 1\},$$

$$\text{then } \boldsymbol{\gamma} = \boldsymbol{\gamma}_3 = \{+1 \;\; -1 \;\; +1 \;\; -1 \;\; +1 \;\; -1 \;\; +1 \;\; -1\}$$

$$\text{if } \mathbf{r} = \{1 \;\; 0 \;\; 0\},$$

$$\text{then } \boldsymbol{\gamma} = \boldsymbol{\gamma}_4 = \{+1 \;\; -1 \;\; -1 \;\; -1 \;\; +1 \;\; -1 \;\; -1 \;\; -1\}$$

$$\text{if } \mathbf{r} = \{1 \;\; 0 \;\; 1\},$$

$$\text{then } \boldsymbol{\gamma} = \boldsymbol{\gamma}_5 = \{+1 \;\; -1 \;\; +1 \;\; +1 \;\; -1 \;\; -1 \;\; +1 \;\; -1\}$$

$$\text{if } \mathbf{r} = \{1 \;\; 1 \;\; 0\},$$

$$\text{then } \boldsymbol{\gamma} = \boldsymbol{\gamma}_6 = \{+1 \;\; -1 \;\; +1 \;\; +1 \;\; -1 \;\; +1 \;\; -1 \;\; -1\}$$

$$\text{if } \mathbf{r} = \{1 \;\; 1 \;\; 1\},$$

$$\text{then } \boldsymbol{\gamma} = \boldsymbol{\gamma}_7 = \{+1 \;\; -1 \;\; +1 \;\; +1 \;\; +1 \;\; +1 \;\; -1 \;\; +1\}. \tag{11}$$

According to (11), the eight rotational modes will be selected according to the changes of binary design variable $\mathbf{r}$. The clockwise or counterclockwise rotational directions of joints in (11), γ_i, can have the two values in (12) while satisfying the geometrical conditions of (8):

$$\gamma_i = \begin{cases} -1: & \text{Cloclwise motion} \\ 1: & \text{Counterclockwise motion} \end{cases} \qquad (i = 1, 2, \ldots, 8). \tag{12}$$

Unlike the rotational direction, the magnitudes of initial joint angle and joint step size angle are parameterized with the integer design variables α and β, respectively. Finally, the binary variables and the integer variables vary from 0 degree to 90 degrees with one degree step which will be used as design variable in this research; the magnitude of the step angle can be smaller or larger but this research adopts this value to verify the effectiveness of the present algorithm:

$$\mathbf{x} = \left[\underbrace{r_1, r_2, r_3}_{\text{binary variable}} \;, \quad \underbrace{\alpha, \beta}_{\text{integer variable}} \right] \tag{13}$$

$$\left(r_i \in [0, 1] \;\text{ for } i = 1, 2, 3, \;\; \alpha, \beta = 0^\circ, 1^\circ, \ldots, 89^\circ, 90^\circ\right).$$

The above rotational directions of joints, the initial joint angle, and the joint step size angle in (11) and (13) are depicted in Figure 11. Note that last three rotational modes, $\boldsymbol{\gamma}_5$, $\boldsymbol{\gamma}_6$,

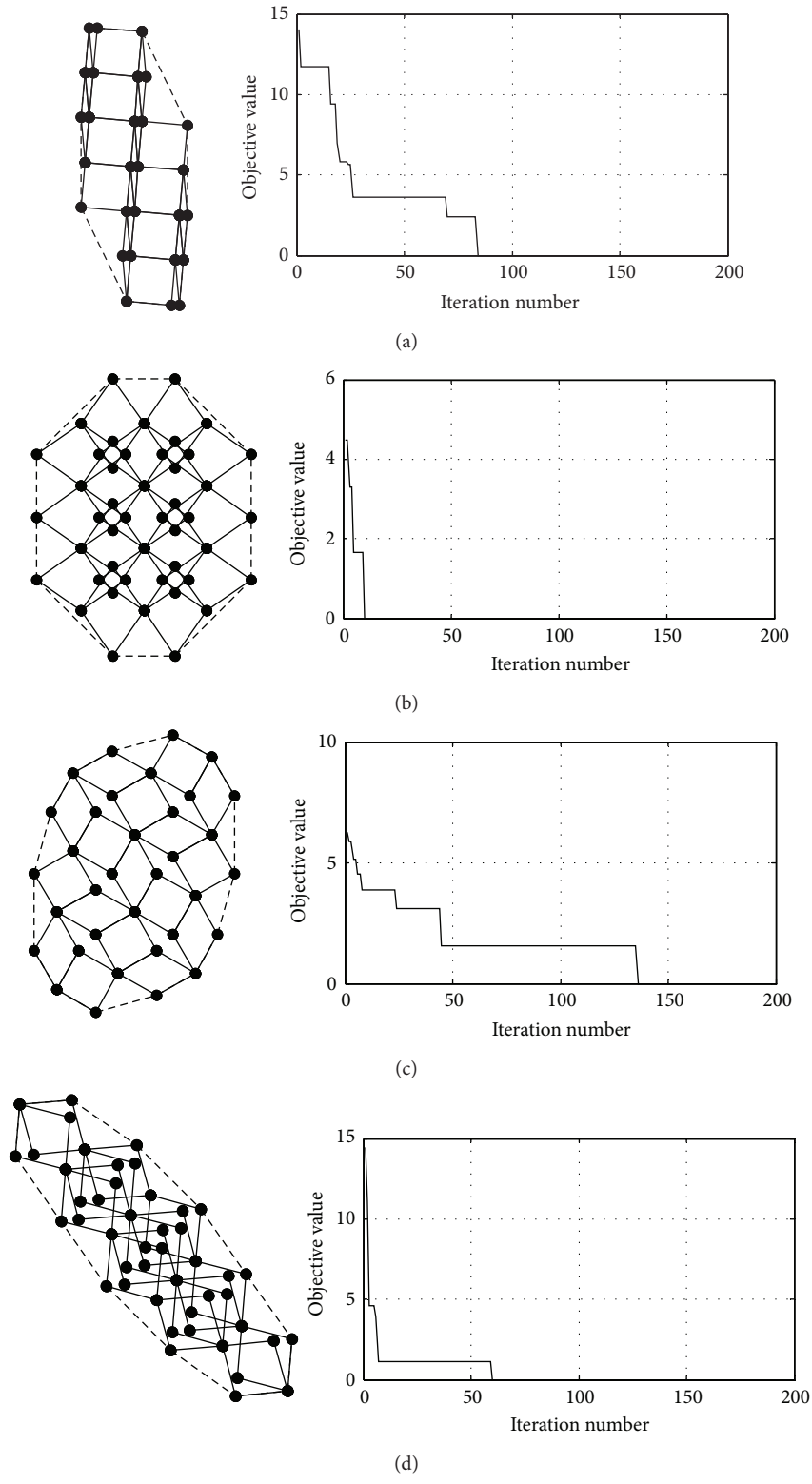

FIGURE 18: Optimization results for a 3 by 2 foldable structure. (a) An optimized foldable structure for the target area 1 and its convergence history ($\mathbf{x} = [1, 1, 1, 45, 40]$), (b) an optimized foldable structure for the target area 2 and its convergence history ($\mathbf{x} = [0, 1, 1, 30, 5]$), (c) an optimized foldable structure for the target area 3 and its convergence history ($\mathbf{x} = [1, 0, 1, 45, 15]$), and (d) an optimized foldable structure for the target area 4 and its convergence history ($\mathbf{x} = [0, 0, 1, 50, 35]$).

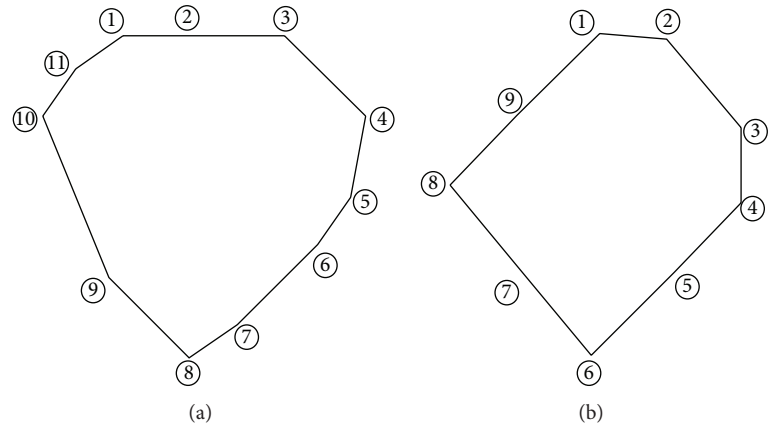

Figure 19: (a) Target area 1 and (b) target area 2 of irregular foldable structures assemblies.

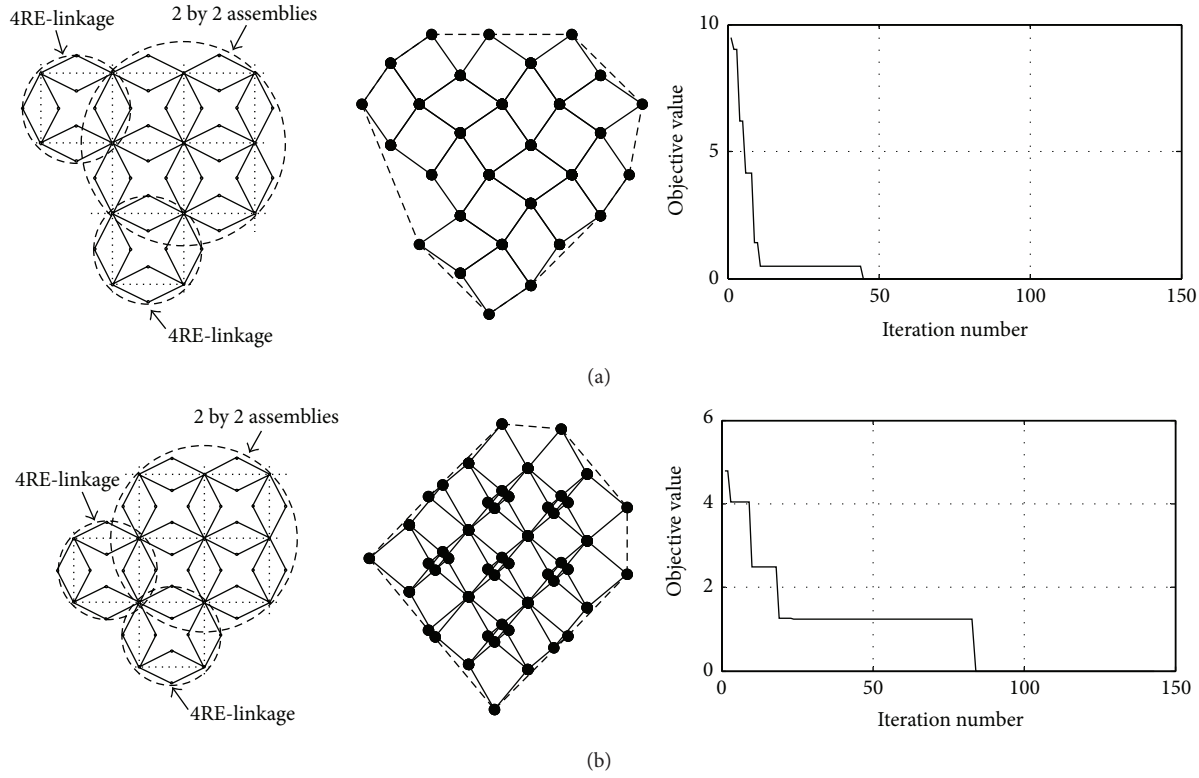

Figure 20: Optimization result of numerical examples for foldable structure using irregular assemblies. (a) Assemblies of foldable structure, foldable structure for the target area 1, and convergence history ($\mathbf{x} = [1, 1, 0, 45, 40]$). (b) Assemblies of foldable structure, foldable structure for the target area 2, and convergence history ($\mathbf{x} = [1, 0, 0, 35, 5]$).

and $\boldsymbol{\gamma}_7$, are valid only when $\alpha = 45^\circ$. Therefore if one of last three rotational modes is selected and $\alpha \neq 45^\circ$, we forced the objective value to have large value, 10^6, to avoid finding wrong solution which cannot satisfy geometrical configuration constraints in (5).

3.2. Outer Joint Detection by the Delaunay Triangulation. It is crucial to find out the outer joints determining the outline of a foldable structure efficiently and effectively. To do this, a new technique based on the Delaunay triangulation is developed. To make it clear, let us consider a foldable structure in Figure 12(a) which may be regarded as one design obtained during an optimization process and its Delaunay triangulation is shown in Figure 12(b). After this Delaunay triangulation, the information of the edges of the triangles is utilized to find out the joints defining outlines. In other words, we can select some edges of triangles which are shared by only one triangle as shown in Figure 12(c) for the outline edges and the joints defined by the edges as shown in Figure 12(b).

(a) (b)

Figure 21: Arbitrary target area. (a) A hole creation by using hammer and (b) the created hole.

3.3. Optimization Problem Formulation. To find out the optimal design parameters of (13) with which a foldable structure covers an arbitrary shaped area, a proper optimization problem should be formulated. To achieve this, this research chooses the rotational directions and the rotational magnitudes are optimized with the following optimization formulation. The objective function is to minimize the summation of the distance values between each reference point of the target area and its closest outer joint of a foldable structure as follows:

$$\begin{aligned}
&\text{Find} \quad \mathbf{x} = [\gamma_1, \gamma_2, \ldots, \gamma_8, \beta] \\
&\text{Min.} \quad \sum_{i=1}^{n} \min\left(l_{i,1}, l_{i,2}, \ldots, l_{i,m}\right), \\
&\qquad \text{where} \\
&\qquad l_{i,j} = \sqrt{\left(x_{\text{ref},i} - x_{\text{current},j}\right)^2 + \left(y_{\text{ref},i} - y_{\text{current},j}\right)^2}, \\
&\qquad i = 1, 2, \ldots, n, \quad j = 1, 2, \ldots, m, \\
&\qquad\qquad \mathbf{x} = \left[\underbrace{\gamma_1, \gamma_2, \ldots, \gamma_8}_{\text{Rotatary direction of joint}} \quad , \underbrace{\beta}_{\text{Angle}}\right], \\
&\left(\gamma_i \in [0, 1] \ \text{ for } i = 1, \ldots, 8, \ \beta = [0^\circ, 1^\circ, \ldots, 89^\circ, 90^\circ]\right).
\end{aligned} \tag{14}$$

The distance between the ith reference joint and the jth outer joint is denoted by $l_{i,j}$. The total number of the reference points defining the outline of the target area and the total number of the outer joints are denoted by n and m, respectively. See Figure 13 for the meanings of the distance definition and the objective function. Obviously before an optimization process, the objective function has a large positive value. As an optimization goes by in the framework of the genetic algorithm, the objective function is decreased and its corresponding area will be similar to the target area. Here note that there can be many local and global optimum solutions. Therefore the population based optimizer can be one of the optimizers. And the initial configurations of the rhombic elements influence the optimization processes. For an example, to cover some areas, we can use 2 by 2, 3 by 2, or other rhombic elements. Therefore it should be determined by an engineer what kind of rhombic elements is adopted. Furthermore the target points should be chosen considering the type of the employed rhombic element.

To successfully solve the optimization problem with the binary and the integer design variables, a genetic algorithm (GA) is one of the most suitable algorithms for the structural optimization of foldable structure [15].

3.4. Optimization Formulation: Genetic Algorithm. The design variables of the present design method are binary and integer design variables; a genetic algorithm (GA) is one of the most suitable algorithms for the optimum design optimization of foldable structure [15]. Note that the GA algorithm should optimize the binary design variables parameterizing the rotational directions of joints and the integer design variable parameterizing the step size of angle which requires some extensions of generic genetic algorithm. In this research, we adopt a GA code implemented in Matlab as shown in Figure 14.

4. Design Optimization Examples

4.1. The 2 by 2 Foldable Structure Design Examples. For the first numerical example, the optimized directions and angles of a 2 by 2 foldable structure covering the four target areas in Figure 15 are optimized. The number of individuals and mutation rate for the genetic algorithm are set to 100 and 0.09, respectively. The target areas are randomly chosen by manipulating the 2 by 2 foldable structure before optimization in order to guarantee the existence of optimal solutions. As expected, the various shapes can be covered by the foldable structure and the detail positions of the four designs are given in Table 1. The developed optimizations linked with the foldable mechanism analysis in the framework of the

Table 1: The positions of the nodal points of the example in Figure 15.

	Target area 1		Target area 2		Target area 3		Target area 4	
	x	y	x	y	x	y	x	y
1	−6.664	10.51	−7.348	7.348	−0.886	11.32	−8.822	8.822
2	−1.026	10.51	−6.572	10.25	0.521	10.67	−6.364	10.54
3	1.793	9.483	−2.898	12.37	2.298	5.785	−3.131	9.366
4	2.819	6.664	0.776	8.693	2.298	1.928	0.544	5.691
5	0	0	0.776	2.898	−1.928	−2.298	1.721	2.457
6	−6.664	−2.819	0	0	−3.336	−1.641	0	0
7	−9.483	−1.793	−0.776	−2.898	−5.113	3.241	−2.457	−1.721
8	−10.51	1.026	−2.329	−2.898	−5.113	7.098	−5.691	−0.544
9	−10.51	6.664	−5.227	−2.121	—	—	−9.366	3.131
10	—	—	−8.125	4.451	—	—	−10.54	6.364

Table 2: The positions of the nodal points of the example in Figure 17.

	Target area 1		Target area 2		Target area 3		Target area 4	
	x	y	x	y	x	y	x	y
1	−6.239	15.47	−5.162	12.78	−1.5	15.99	−15.44	16.57
2	−5.716	15.47	−1.721	12.78	1.098	14.49	−12.45	16.83
3	−2.727	15.20	2.457	8.604	2.598	11.89	−8.685	14.19
4	0.261	8.966	2.457	5.162	2.598	6.696	−5.011	10.52
5	0.261	2.989	2.457	1.721	1.5	2.598	−2.375	6.754
6	0	0	−1.721	−2.457	0	0	0.261	2.989
7	−0.261	−2.989	−5.162	−2.457	−2.598	−1.5	0	0
8	−0.784	−2.989	−9.340	1.721	−6.696	−2.598	−2.989	−0.261
9	−3.773	−2.727	−9.340	5.162	−9.294	−1.098	−6.754	2.375
10	−6.762	3.512	−9.340	8.604	−10.79	1.5	−10.43	6.049
11	−6.762	9.489	—	—	−10.79	6.696	−15.70	13.58
12	−6.500	12.48	—	—	−9.696	10.79	—	—
13	—	—	—	—	−8.196	13.39	—	—
14	—	—	—	—	−5.598	14.89	—	—

constraint force method are conducted in Figure 16. As shown the four designs covering the target areas can be found successfully with the genetic algorithm. These examples prove that the developed algorithm can find out the optimum designs covering target areas.

4.2. The 3 by 2 Foldable Structure Design Examples. In addition to the optimum design of the 2 by 2 foldable structure, the developed algorithm can easily consider a more general foldable structure. To show this feature, the 3 by 2 foldable structure is chosen as a basic foldable structure and the optimization problems of Figure 17 are considered. As in the first numerical examples, the target areas are chosen by manipulating the 3 by 2 foldable structure a priori and the number of individuals and mutation rate for the genetic algorithm are set to 100 and 0.09, respectively. Compared with the covered areas of the 2 by 2 foldable structure, that of the 3 by 2 foldable structure can represent more detailed and smoothed structures of the target areas as expected. The design optimization results for four target areas and the optimization convergence history are shown in Figure 18. After the optimization, all of the objective values for four problems are converged to zero. The detail positions of the four mechanisms are given in Table 2.

4.3. The Design Examples Using Arbitrary Assemblies. At the first and the second numerical examples, the applications of the 2 by 2 and the 3 by 2 foldable mechanisms are solved by the present approach. Through these two numerical examples, we observed that it is possible to find out some optimal foldable mechanisms covering some complex target areas. Now to see the applicability of an arbitrarily chosen mechanism, the target areas of Figure 19 are considered. Unlike the previous two examples, the areas are chosen for the arbitrary assemblies of the rhombic elements. And the optimum designs are shown in Figure 20.

4.4. Realization of Foldable Structure Design. The previous examples show some benchmark problem of the foldable structures and the present optimization algorithm. To show the validity of the present design strategy for real application, we create an arbitrary shaped area by breaking a cap of a plastic product in Figure 21. Then the outline of the hole is scanned and the target area is extracted in Figure 22(a); the

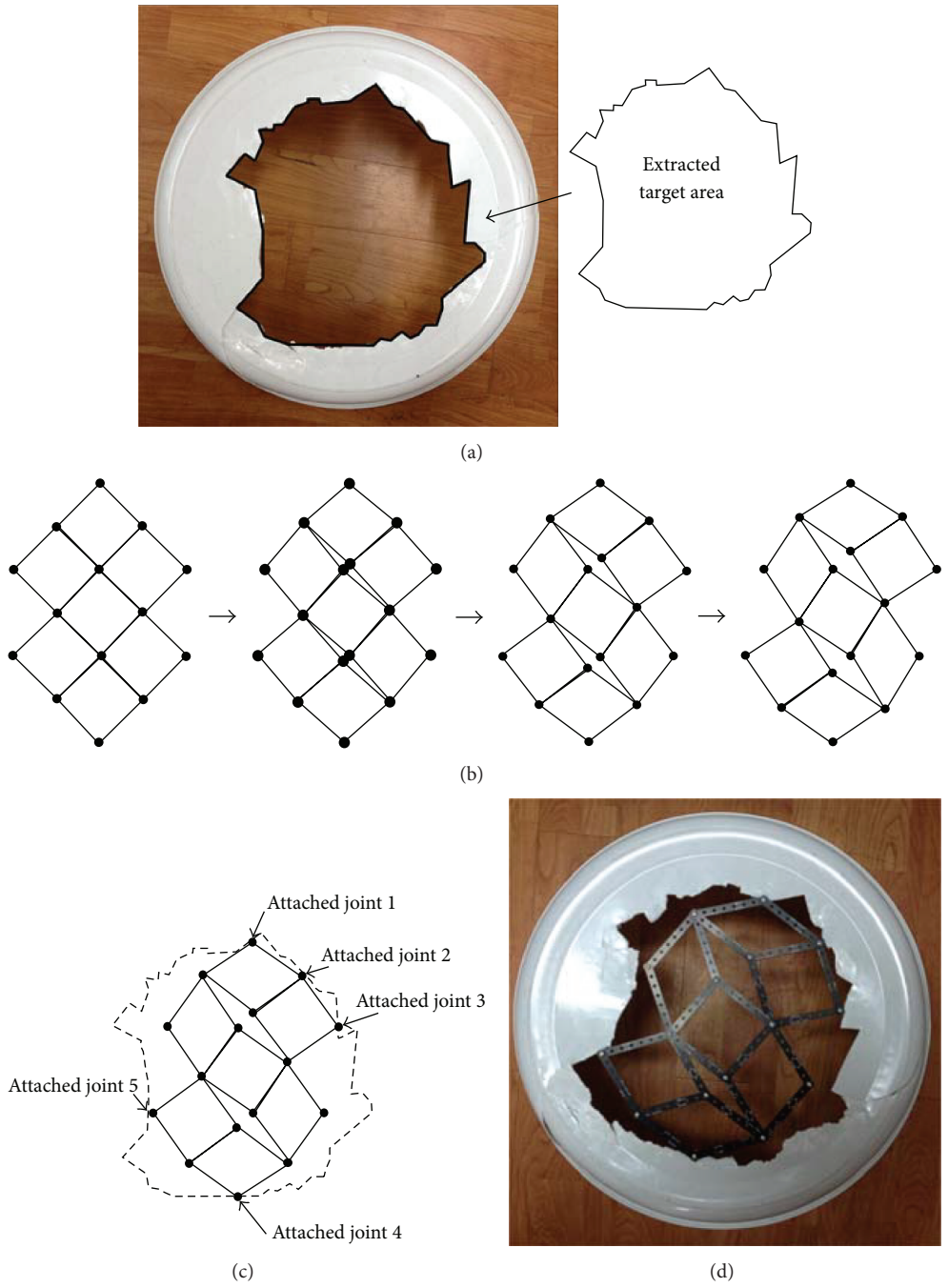

FIGURE 22: Optimization result of foldable structure for arbitrary area. (a) The extracted target area, (b) the foldable motions of the 2 by 1 assemblies, (c) the foldable structure for the target area using 2 by 1 assemblies ($\mathbf{x} = [1, 0, 1, 45, 12]$), and (d) the realized foldable structure for the target area.

key points of the outline can be chosen manually. Here we chose the 2 by 1 foldable structure to cover this break hole. With the present design process, the design of Figure 22(b) can be obtained and its structure is made in Figures 22(c) and 22(d). Due to physical size of a link, we found that the 2 by 1 foldable structure with $\mathbf{x} = [1, 0, 1, 45, 12]$ is the most suitable in covering the hole. If the length of link can be adjustable, a more complex foldable structure can be used for this implementation. This example shows a possible application of the present optimization method.

5. Conclusions

In this paper, we present new design optimization method of foldable structure. The foldable structure is developed to construct light structure which has sufficient stiffness and strength. However, due to complex deformation mobility of foldable structure, it is difficult to find out appropriate deformation mode satisfying actual requirements. Our recent work focused on the design of deformation mobility of foldable structure which covering arbitrary shaped area by

finding appropriate rotational direction of joints and step size angle. To develop new structural optimization method, it is necessary to define appropriate design variables. Through the kinematic analysis of 4RE-linkages, it is found that the deformation mobility can be defined by eight rotational joint and step size angle. Therefore, the mixed design variables which represent the rotational direction of joints as binary design variables and the step size angle as integer design variable are used. Due to two types of design variables, the genetic algorithm treating binary and integer design variables simultaneously is used in this research. The objective function of optimization problem is defined to minimize the sum of distances between target area's reference node point and its closest outer node point of foldable structure. The outer node points of foldable structure are found based on Delaunay triangulation. The usefulness of developed optimization method is verified by successfully designing four kinds of foldable structures covering arbitrary shaped area.

Conflict of Interests

The authors declare that there is no conflict of interests regarding the publication of this paper.

Acknowledgment

This research was supported by the EDISON Program through the National Research Foundation of Korea (NRF) funded by the Ministry of Science, ICT & Future Planning (no. NRF-2014M3C1A6038801).

References

[1] Z. You and S. Pellegrino, "Foldable bar structures," *International Journal of Solids and Structures*, vol. 34, no. 15, pp. 1825–1847, 1997.

[2] O. Benjeddou, O. Limam, and M. B. Ouezdou, "Experimental and theoretical study of a foldable composite beam," *Engineering Structures*, vol. 44, pp. 312–321, 2012.

[3] A. Zanardo, "Two-dimensional articulated systems developable on a single or double curvature surface," *Meccanica*, vol. 21, no. 2, pp. 106–111, 1986.

[4] C. Hoberman, "Continuously rotating mechanisms," 2001.

[5] C. Hoberman, "Folding covering panels for expanding structures," 2004.

[6] C. Hoberman, "Loop assemblies having a central link," 2006.

[7] A. D. Viquerat, T. Hutt, and S. D. Guest, "A plane symmetric 6R foldable ring," *Mechanism and Machine Theory*, vol. 63, pp. 73–88, 2013.

[8] J.-S. Zhao, F. Chu, and Z.-J. Feng, "The mechanism theory and application of deployable structures based on SLE," *Mechanism and Machine Theory*, vol. 44, no. 2, pp. 324–335, 2009.

[9] J.-S. Zhao, J.-Y. Wang, F. Chu, Z.-J. Feng, and J. S. Dai, "Structure synthesis and statics analysis of a foldable stair," *Mechanism and Machine Theory*, vol. 46, no. 7, pp. 998–1015, 2011.

[10] J. Cai, Y. Xu, and J. Feng, "Kinematic analysis of Hoberman's Linkages with the screw theory," *Mechanism and Machine Theory*, vol. 63, pp. 28–34, 2013.

[11] A. B. Kempe, "On conjugate four-piece linkages," *Proceedings of the London Mathematical Society*, vol. S1-9, no. 1, pp. 133–149, 1878.

[12] S. Gina, *Mission Extended to Fix Thermal Blanket*, ABC NEWS, New York, NY, USA, 2007.

[13] F. Tom and G. Daniel, "Oil-pipeline cracks evading robotic "Smart Pigs"," *The Wall Street Journal*, 2013.

[14] H. Tanaka, Y. Shibutani, S. Izumi, and S. Sakai, "Planar mobility modes of 8-bar-jointed structures with a single degree of freedom," *International Journal of Solids and Structures*, vol. 49, no. 13, pp. 1712–1722, 2012.

[15] J. H. Holland, "Genetic algorithms," *Scientific American*, vol. 267, no. 1, pp. 66–72, 1992.